Journal of Power Sources 196 (2011) 6762–6767

Contents lists available at ScienceDirect

Journal of Power Sources

journal homepage: www.elsevier.com/locate/jpowsour

Synthesis and electrochemical property of $LiCoO_2$ thin films composed of nanosize compounds synthesized via nanosheet restacking method

Zhen Quan, Kosuke Iwase, Noriyuki Sonoyama*

Department of Materials Science and Engineering, Nagoya Institute of Technology, Gokiso-cyo, Showa-ku, Nagoya 466-8555, Japan

ARTICLE INFO

Article history:
Received 12 August 2010
Received in revised form 1 October 2010
Accepted 25 October 2010
Available online 3 November 2010

Keywords:
Nanosheet
Electrophoretic deposition
Hydrothermal
High rate discharge performance

ABSTRACT

$LiCoO_2$ thin films with nanosize particles were synthesized on Au substrates by nanosheet restacking method and subsequent hydrothermal reaction which needs less cost than the vacuum deposition methods. The grain size of $LiCoO_2$ films estimated by XRD reflection was about 15 nm that was independent of the thickness of precursor cobalt hydroxide film. Comparing the rate performance of the thin films with various thickness, the optimum performance was obtained by the thin film with 5 min deposition time: 62% of the capacity was held at 400 C-rate compared with that at 20 C-rate. The results of AC-impedance analysis of electrode reaction indicate that the high rate capability of the $LiCoO_2$ film is obtained by the small grain size and large surface area of $LiCoO_2$ thin film with nano size particles.

1. Introduction

Rechargeable thin film batteries have attracted much attention of many researchers and market as important power source for various small electronic devices such as smart card, microelectromechanimal system, and so on. Recently, various kinds of synthesis methods of lithium battery cathode material thin films, such as sol–gel method [1], aerosol flame deposition (AFD) [2], sputtering [3] and pulsed laser deposition (PLD) [4] have been developed. Among these methods, sol–gel and AFD method can produce cathode films with lower cost. However, the performance of the film is not much improved from that of the bulk materials in spite of the comparatively smaller particle size (30–120 nm). Contrary to these methods, it was reported that high performance cathode films can be obtained by using the vacuum deposition methods [3,4]. Especially, cathode thin film synthesized by PLD method is composed of extremely small particle (10–30 nm) with high density and high surface flatness [4,5]. This film shows excellent electrochemical performance: Matsumura et al. reported that $LiMn_2O_4$ thin film synthesized by PLD method shows charge–discharge ability even at over 500 C-rate [4]. The weak point of this film is synthesis cost for most of vacuum deposition methods require highly vacuum condition. This vacuum process raises the total fabrication cost of thin film cell.

Besides the study of such thin films, synthesis method of nanosize fine grain of powder cathode material has been developed in the last decade [5–8]. In order to obtain higher charge–discharge rate capability, either shorter Li-ion diffusion length, d, or higher chemical Li-ion diffusion coefficient, D_{Li} is necessary. Commercial cathodes with long d (ca. 1 μm) are not suitable for high power batteries, while particles with nanometer order size d should contribute to achieve the rate capability. As an example, Okubo et al. reported that an excellent high rate capability was observed in nanocrystalline $LiCoO_2$ with an appropriate particle size of 17 nm, synthesized by hydrothermal method [5].

Lately, a variety of unilamellar two-dimensional crystallites with chemically delaminating a layered compound into molecular single layers have been actively studied [10,11]. The resulting elementary layers so called "nanosheets", with it own thickness of a nano- or sub nanometer, have well-defined composition and highly crystalline nature as a single layer material. Using the nanosheets of metal oxide like TiO_2 [6] and MnO_2 [7], new types of metal oxide layered compounds were synthesized and applied as the electrodes of lithium battery. These nano-sheets show charge–discharge feature as cathode materials.

In the present study, $LiCoO_2$ films composed of nano size compounds attempted to be synthesized by electrochemical deposition of nanosheet and subsequent hydrothermal treatment, and electrochemical property of obtained films were examined.

2. Experimental

The procedure of the synthesis of $LiCoO_2$ films was summarized in Scheme 1. $Co(OH)_{1.72}(DBS)_{0.27}\cdot 1.06H_2O$ was prepared by anion exchange reaction with sodium dodecylbenzenesulfonate (NaDBS) (0.05 M, Kishida chemical) solution at 70 °C, starting

* Corresponding author.
E-mail address: sonoyama@nitech.ac.jp (N. Sonoyama).

0378-7753/$ – see front matter © 2010 Elsevier B.V. All rights reserved.
doi:10.1016/j.jpowsour.2010.10.076

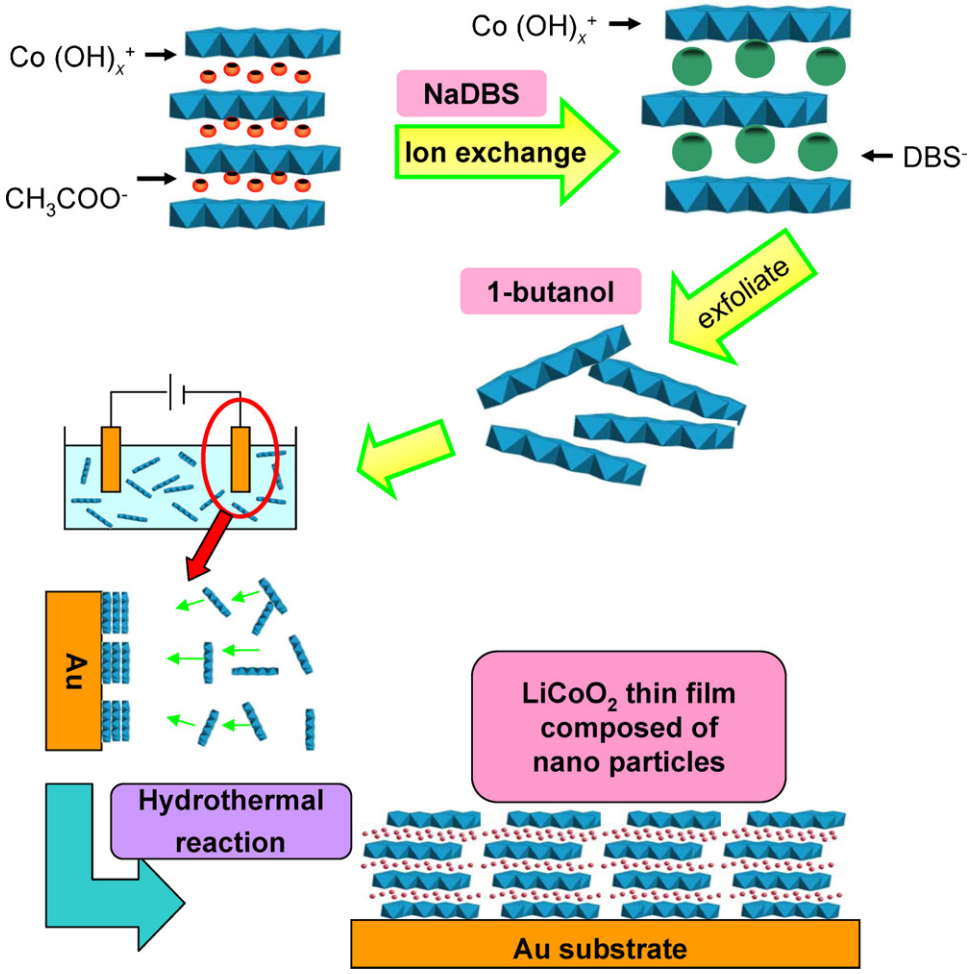

Scheme 1. Synthesis of nanosize $LiCoO_2$ by nanosheet restacking and subsequent hydrothermal method.

from layered compound $Co(OH)_{1.62}(CH_3COO)_{0.38}\cdot 0.53H_2O$ [8]. The precipitate was filtered, dried, and then mixed with 1-butanol (99.5%, Kishida chemical) to give colloidal suspensions of cobalt hydroxide nanosheets. Restacked nanosheets were obtained by electrophoretic deposition (EPD) in the colloidal suspensions with the current density of 20 μA/cm^2 controlled by galvanostat (Hokuto HABF-501) for 5, 15, 30, 60 and 240 min on Au substrates (10 mm × 10 mm). For the observation of the surface morphology of the deposited nano sheet, 10 s deposited film on the Au coated mica substrates were used. $LiCoO_2$ thin films were prepared by hydrothermal reaction of restacked nanosheet films in 1 M LiOH solution at 170 °C for 12 h. After the hydrothermal reaction, the as-prepared $LiCoO_2$ thin films were annealed at 500 °C for 1 min in air to improve crystallinity.

The crystal structure of the thin films was characterized by X-ray diffraction (Rigaku RAD-C) using Cu Kα1 radiation in steps of 0.03° for the range of 10–90°. Raman spectra were recorded on a Laser Raman Spectroscopy (JASCO NR-1100) in the range of 200–800 cm^{-1}, using Ar ion laser (λ = 514 nm).

The morphology of thin film was observed by scanning electron microscope (JEOL JSM-5610). Elemental analysis for the $Co(OH)_x$ nanosheet is carried out using EDS (JOEL JSM-7001FF) equipped with SEM system. The surface areas of the thin films were measured by laser microscope (KEYENCE VK-9700). AFM measurement was performed by JEOL JSPM-5200 SPM microscope in AC mode, using Si cantilevers tip with the spring constant 42 N/m.

Electrochemical measurement of the $LiCoO_2$ thin film was performed using self designed cell for thin film electrode at 25 °C. The main body of the cell with the shape of hollow cuboid is made by Diflon. A small hole with the area of 0.64 cm^2 is on the main body and opposite side is opened. Anode and cathode are fixed on the two stainless steel plates, and located at two opposite sides of the main body so that electrodes contact with the electrolyte. Lithium metal was used as anode and 1 M solution of $LiPF_6$ in EC:DEC (1:1, v/v) was used as the electrolyte. Charge–discharge measurement was carried out in the potential range between 3.5 V and 4.3 V by a potentio-galvanostat (Hokuto HA-501) and a function generator (Hokuto HB-105). Electrochemical impedance spectroscopy measurements of the cells were performed using an impedance analyzer (Solatron 1255). The frequency range was from 10 mHz to 1 MHz with the applied voltage of 10 mV. The voltage imposed on the electrode was controlled by potentiostat (Solatron 1280C).

3. Results and discussion

Fig. 1 shows XRD patterns for the precursor and products in the synthesis process (Scheme 1). As were seen in Fig. 1(a), the interlayer reflections of $Co(OH)_{1.72}(DBS)_{0.27}\cdot 1.06H_2O$ shifted to lower angle by exchanging CH_3COO^- ion to DBS^- ion, for the distance between cobalt hydroxide layers increased by exchanging to bulky anion. By dispersing DBS^- exchanged cobalt hydroxide, $Co(OH)_x$ nanosheets emulsion can be obtained. In Fig. 1(b), XRD pattern for hydrothermal treated $Co(OH)_x$ films after 240 min EPD was shown. 0 0 3, 1 0 1, 1 0 5 and 0 0 9 reflections can be observed and agreed with the position of $LiCoO_2$ (ICSD No. 29225), though the reflections of impurities phase containing Co_3O_4 were also observed.

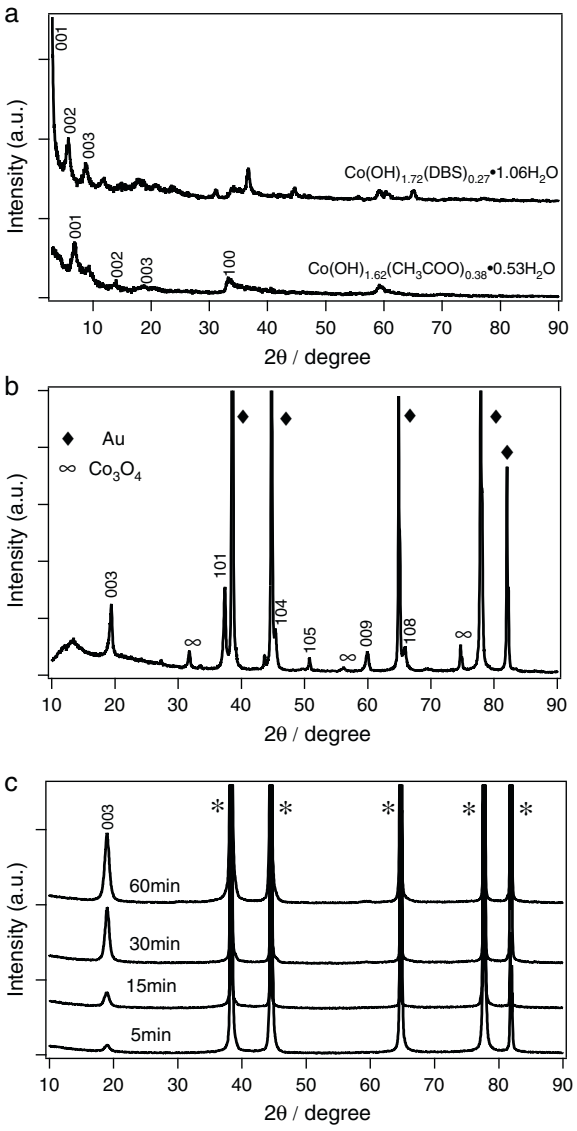

Fig. 1. (a) XRD patterns for layered compounds before and after ion exchange. (b) XRD pattern of $LiCoO_2$ thin film synthesized by hydrothermal reaction after electroplating for 240 min. (c) XRD patterns of the $LiCoO_2$ thin film synthesized from precursor cobalt hydroxide films with different cathodic electroplating period. *: Au substrate.

Fig. 1(c) is the XRD patterns for $LiCoO_2$ films electroplated with deposition time of 5, 15, 30 and 60 min. Comparing with pattern in Fig. 1(b), for the films with shorter time electroplated, only the 0 0 3 reflection of $LiCoO_2$ can be observed because of the reflection of Au substrate that locates near other reflections of $LiCoO_2$. The grain size, estimated from the full width at half maximum of 0 0 3 reflections of $LiCoO_2$ thin films synthesized on Au substrates, are about 14.8, 14.9, 16.9 and 15.6 nm, respectively. This indicates the grain size of the thin films is independent of the thickness of precursor cobalt hydroxide films. These crystallite sizes were near the particle size of nanosize $LiCoO_2$ powder (17 nm) synthesized under the same hydrothermal reaction condition reported by Okubo et al. [5].

In Fig. 2, Raman scattering spectrum for thin film hydrothermal treated after 5 min EPD was shown. Characteristic scatterings those can be assigned to A_{1g} and E_g of $LiCoO_2$ were observed at around 484 and 594 cm^{-1}, respectively. Scatterings of Co_3O_4, which were reported to exist as impurity in the $LiCoO_2$ thin films in previous works [2,9], were also observed. However, the amount of the

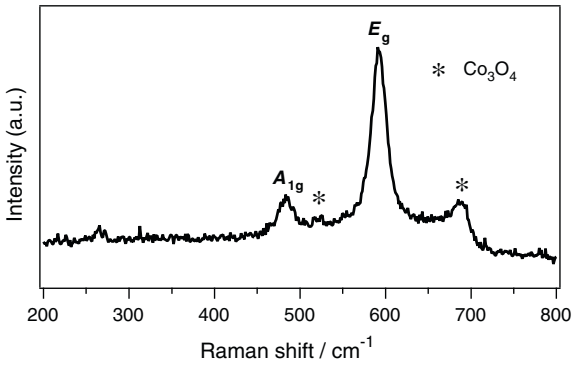

Fig. 2. Raman spectrum for $LiCoO_2$ thin film electroplated for 5 min on Au substrate.

Co_3O_4 in the thin films was considered to be very low because XRD reflection of Co_3O_4 was not found in the thinner films (Fig. 1(c)). From these data, it was concluded that $LiCoO_2$ film composed of the nano size grain can be synthesized via a cobalt hydroxide nanosheet electroplating and subsequent hydrothermal treatment.

Fig. 3(a) shows SEM image of deposited compound on the surface of Au coated mica substrate after 10 s electro-deposition. A disc like sheet with a diameter of about 100 nm was observed. In Table 1, the composition of this sheet analyzed by EDS was listed. The deposited sheet is mainly consisted with cobalt, carbon, sulfur and oxygen. This composition agreed with that of DBS^- ion exchanged $Co(OH)_x$ sheet. AFM image of the surface of the film with deposition time of 10 s was shown in Fig. 3(b). Large masses with height of 110 nm and scaly sheets with height of 30 nm were found. Scaly sheets would be the deposited $Co(OH)_x$ nanosheets that were observed by SEM (Fig. 3(a)) and larger masses would be the clusters of $Co(OH)_x$ sheets that were not fully dispersed in the solution. Fig. 3(c) and (d) shows the SEM images of the surface of the films with 5 min electro-deposition before and after the hydrothermal treatment. Before hydrothermal treatment, the configuration of the stacked nanosheets can be confirmed. After the treatment, aggregates of spherical particles were found whereas the secondary particles can be seen that consist of grain with the size of about 10–20 nm. The size of the primary particles is almost consistent with the estimated grain size from the half band width of X-ray reflection (Fig. 1). Fig. 3(e)–(h) shows the surface morphologies of $LiCoO_2$ films with different deposition time. Evident surface morphology change was perceived with the deposition time. For the films with shorter deposition time (5–15 min), the surface of film was much rugged with three dimensional surface structure, whereas the denser and smoother surface was observed for the films with longer deposition time (30–60 min).

The charge–discharge curves for the $LiCoO_2$ film with the deposition time of 5 min were shown in Fig. 4(a). Evident plateaus were observed both in the charging and discharging processes. Okubo et al. [5] reported that with decreasing the particle size of $LiCoO_2$, the plateaus became indistinct in the region of the size below 10 nm. They explained this reason that the impurity phase Co (II) compounds, that are contained at the surface of $LiCoO_2$ increases with the increasing the surface area by the size reduction

Table 1
Composition of $Co(OH)_x$ nanosheet analyzed by EDS.

Element	wt (%)	at. (%)
Co	48.75	20.94
C	14.07	29.65
O	28.77	45.51
S	4.26	3.37
Au	4.15	0.53

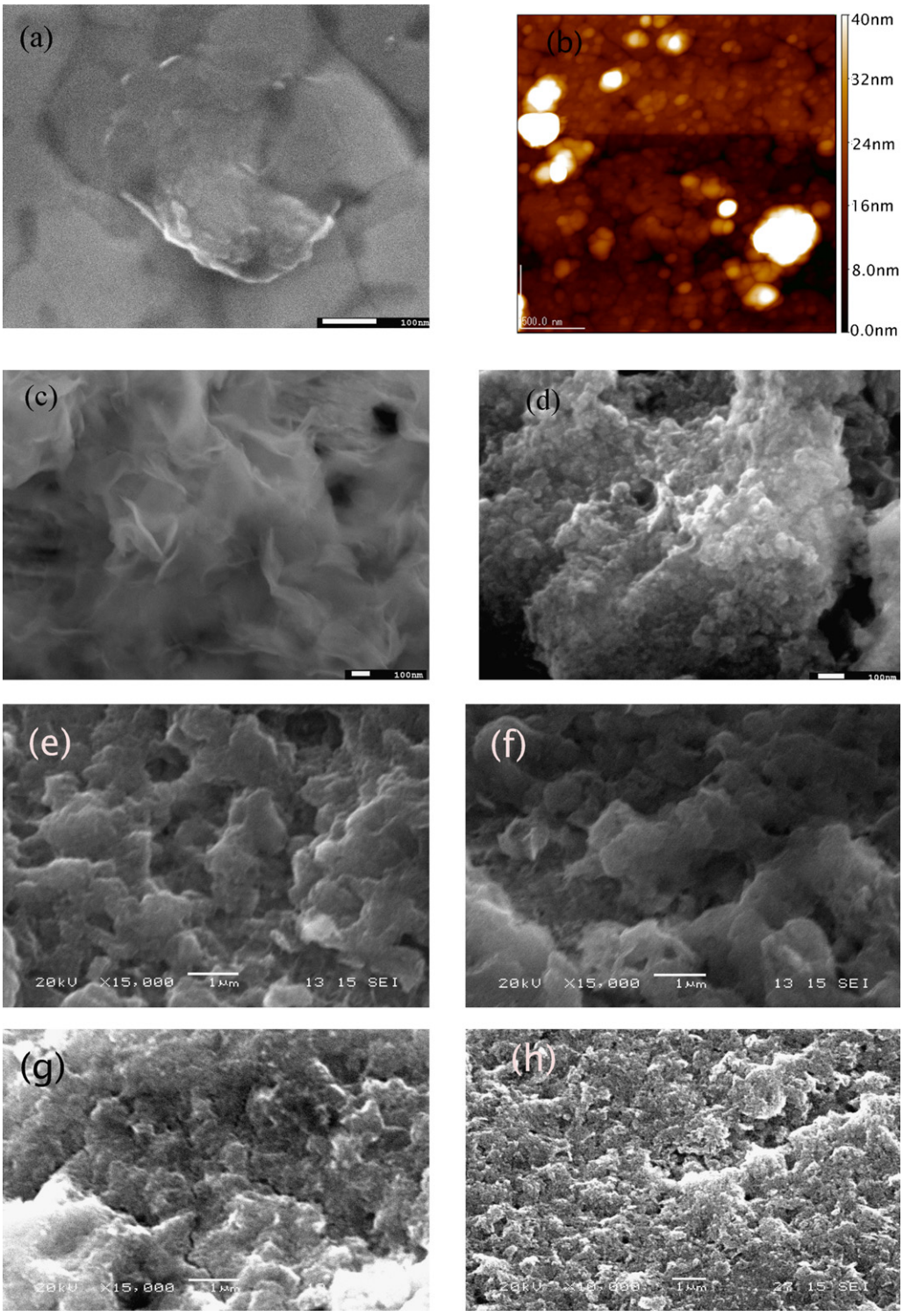

Fig. 3. (a) SEM image of deposited compounds on the surface of Au coated mica substrate after 10 s electro-deposition. (b) AFM image of cobalt nanosheets deposited on Au substrate with 10 s deposition time. (c) and (d) SEM images of the surface of the films with 5 min electro-deposition (c) before and (d) after the hydrothermal treatment. (e)–(h) The surface morphologies of $LiCoO_2$ films with different deposition time. (e) 5 min, (f) 15 min, (g) 30 min, and (h) 60 min.

of $LiCoO_2$. In the present study, the particle size estimated from XRD is 14–17 nm. This size is almost consistent with the most appropriate size of $LiCoO_2$ nano particle Okubo et al. reported: around 17 nm [5]. In the discharging process, ohmic potential drop was observed with raising discharge rate. As shown in Table 2, increasing C-rate from 20 C to 200 C for the $LiCoO_2$ thin film with the deposition time of 5 min, the discharge potential drop was 0.12 V, whereas the same ohmic potential drop occurred by raising the C-rate from 3 C to 21 C for the film with the deposition time of 60 min. This result suggests that electric conductivity decreases with the increasing deposition time.

In Fig. 4(b), relationship between the discharge rate and the utilization efficiency of discharge capacity for $LiCoO_2$ thin films with various thickness was plotted, where the capacity with the current 10 μA is assumed to be obtained with 100% utilization efficiency. For the $LiCoO_2$ films with lower thickness (5 and 15 min deposition),

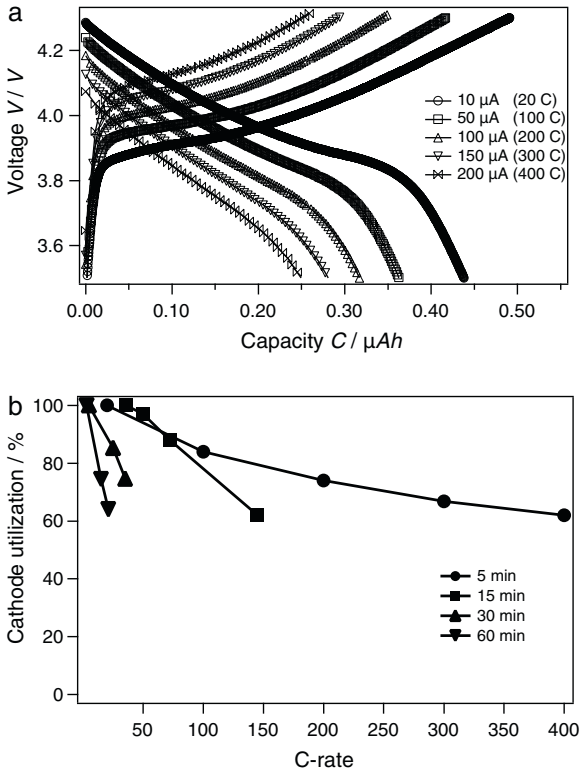

Fig. 4. (a) Charge–discharge curves of 5 min deposited sample at various current and (b) the relationship between the utilization efficiency of the discharge capacity and discharging rate for $LiCoO_2$ film with various thicknesses.

showed good rate performance. Especially, film with 5 min deposition sustained 74% efficiency over 200 C-rate. $LiCoO_2$ powder with nano particle size was reported to show high rate performance: about 63% with 100 C-rate [5]. Increasing the deposition time, for the $LiCoO_2$ film in the present study, utilization efficiency steeply decreased with the increase in the C-rate. This steep decrease in utilization efficiency with deposition time is presumed to be caused by the decrease in electric conductivity, as was described above, because no conducting aid was added in the fabrication process. Despite considering these factors, the difference between the films with deposition time of 15 and 30 min appears to be too large. For the analysis of this electrode reaction, AC impedance spectroscopy measurements were carried out.

In Fig. 5, Nyquist plots of $LiCoO_2$ film on Au substrate with the 5 min deposition time in the frequency range 10^{-2} to 10^{6} Hz at various potentials in the discharge process are shown. At the potential of 3.6 V, only blocking electrode behavior was observed. Above 3.9 V, two depressed semi-circles appeared in the high frequency region and a straight line with 45° slope was obtained in the lower frequency region. The semi-circles at high frequency could be due to the solid electrolyte interface and charge-transfer resistance [9], respectively. The straight line of 45° slope is related to Warburg region where the transition process shifts from charge transfer control to diffusion control. The obtained impedance spectra were analyzed using the equivalent circuit shown in the inset

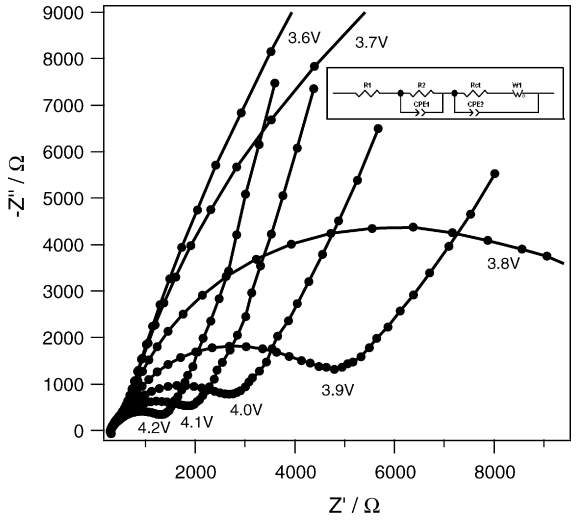

Fig. 5. Nyquist plots for $LiCoO_2$ film on Au substrate with 5 min deposition time at various voltages.

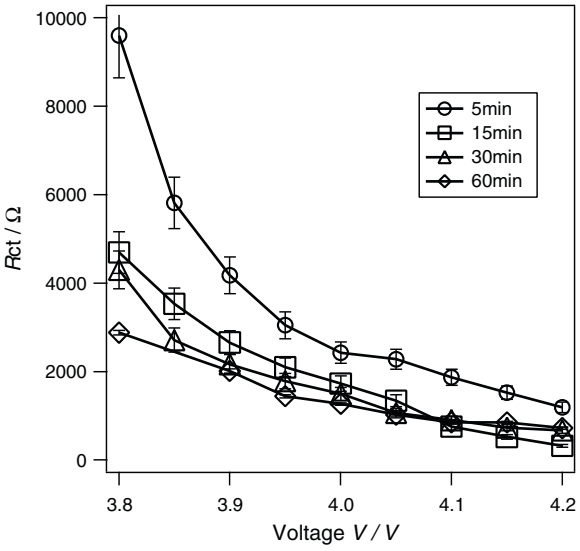

Fig. 6. Charge-transfer resistance R_{ct} of $LiCoO_2$ thin films at various voltages.

of Fig. 5. The relationship between the charge-transfer resistance R_{ct} estimated from the Nyquist plots and the imposed voltage on the $LiCoO_2$ films was shown in Fig. 6. For all films, R_{ct} increased with decreasing the potential. The extent of R_{ct} increase was largely dependent on the film thickness: thinner film trends to show higher R_{ct} at the lower voltage region. In Table 3, the diffusion constants of lithium ion estimated from the AC impedance spectra at 4.2 V were listed. As previous works [10–12] reported that D_{Li} values measured by EIS were in the range of 10^{-9} to 10^{-13} $cm^2\,s^{-1}$, it is difficult to determine the accurate value of the diffusion constants of thin film. Because of EIS method contains some error for calculating the diffusion constants, it is not reliable and can only be

Table 2
The relationship between increased discharge C-rate and ohmic potential drop.

Cathodic electroplating time	The change of the C-rate	Ohmic drop (V)
5 min	20 C to 200 C	0.12
15 min	36 C to 108 C	0.12
30 min	7 C to 50 C	0.11
60 min	3 C to 21 C	0.13

Table 3
The Li-ion chemical diffusion coefficient of $LiCoO_2$ thin film with various thicknesses.

Cathodic electroplating time	D_{Li} by EIS ($cm^2\,s^{-1}$)
5 min	1.66×10^{-12}
15 min	4.80×10^{-12}
30 min	1.16×10^{-11}
60 min	8.01×10^{-12}

considered as the apparent value. In the present work, although the thin film with electroplating 30 min deposition shows highest value, these estimated values seems cannot be used for discussion of diffusion constant dependence on the film thickness for the error they contain. In the present stage, D_{Li} seems to be independent on the film thickness, because the size of particle that consists the film is almost the same in any films synthesized in this study. This estimated diffusion constant agreed with that of $LiCoO_2$ nano particle reported by Okubo et al. (9×10^{-13} cm^2 s^{-1}) [13]. This result seems reasonable, considering particle size of these $LiCoO_2$ is almost the same. The higher R_{ct} for thinner films seems ascribable to the surface area of the films that can be confirmed by the observation of surface SEM image (Fig. 3(d)). This larger surface area for thinner $LiCoO_2$ nano particle film is consistent with the rate dependence of the utilization efficiency of discharge capacity (Fig. 3(d)). The surface area ratios of the $LiCoO_2$ films with deposition time of 15, 30 and 60 min which measured by laser microscope were 2.1814, 1.1658 and 1.3882 $\mu m^2/\mu m^2$, respectively. The sample of 15 min showed the largest surface area, as estimated in Fig. 3(f)–(h). The surface area of the thin film with the deposition time of 5 min cannot be measured because a part of Au substrate exposed among the thin film, but it was confirmed that the surface area of the thinner film tends to be larger than the thicker ones. For thinner films, larger surface area of $LiCoO_2$ film with three dimensional construction would make the fast charge-discharge possible. Increasing the film thickness, surface morphology changed smoother and flatter. This morphology change would make the surface area smaller and fast charge–discharge disable.

4. Conclusions

$LiCoO_2$ thin films composed of nano particles can be prepared by nanosheet restacking and subsequent hydrothermal reaction on the Au substrate. We compared the structures and electrochemical behaviors among the films with various thicknesses. Surface morphology of these films observed by SEM for thinner film has three dimensional surface structure, whereas surface of thicker films become flatter. Optimum high rate performance was obtained by the thinnest film with deposition time of 5 min with large surface area. By optimizing of this method, cathode material films with high performance would be obtained with low cost.

Acknowledgments

We thank Prof. Masaki Tanemura (Nagoya Institute of Technology) for the SEM and AFM measurements and also thank to Keyence Corporation for surface area measurement. This work was financially supported by Tokuyama Science Foundation.

References

[1] Q. Wu, W. Li, Y. Cheng, Z. Jiang, Mater. Chem. Phys. 91 (2005) 463–467.
[2] T. Lee, K. Cho, J. Oh, D. Shin, J. Power Sources 174 (2007) 394–399.
[3] J.-K. Lee, S.-J. Lee, H.-K. Baik, H.-Y. Lee, S.-W. Jang, S.-M. Lee, Electrochem. Solid-State Lett. 2 (1999) 512–515.
[4] T. Matsumura, N. Imanishi, A. Hirano, N. Sonoyama, Y. Takeda, Solid State Ionics 179 (2008) 2011–2015.
[5] M. Okubo, E. Hosono, J. Kim, M. Enomoto, N. Kojima, T. Kudo, H. Zhou, I. Honma, J. Am. Chem. Soc. 129 (2007) 7444–7452.
[6] S. Suzuki, N. Sakai, M. Miyayama, Key Eng. Mater. 388 (2009) 37–40.
[7] Wang, K. Takada, A. Kajiyama, M. Onoda, Y. Michiue, Zhang, M. Watanabe, T. Sasaki, Chem. Mater. 15 (2003) 4508–4514.
[8] L. Poul, N. Jouini, F. Fievet, Chem. Mater. 12 (2000) 3123–3132.
[9] P.J. Bouwman, B.A. Boukamp, H.J.M. Bouwmeester, P.H.L. Notten, J. Electrochem. Soc. 149 (2002) A699–A709.
[10] H. Xia, L. Lu, G. Ceder, J. Power Sources 159 (2006) 1422–1427.
[11] J. Xie, N. Imanishi, A. Hirano, M. Matsumura, Y. Takeda, O. Yamamoto, Solid State Ionics 178 (2007) 1218–1224.
[12] J. Xie, N. Imanishi, T. Matsumura, A. Hirano, Y. Takeda, O. Yamamoto, Solid State Ionics 179 (2008) 362–370.
[13] M. Okubo, E. Hosono, T. Kudo, H.S. Zhou, I. Honma, Solid State Ionics 180 (2009) 612–615.